An Experimental Study of Aerodynamic Drag on High-speed Train

Hyeok-bin Kwon*
Research Assistant, Department of Aerospace Engineering, Institute of Advanced Machinery Design, Seoul National University
Dong-ho Lee
Professor, School of Mechanical and Aerospace Engineering, Seoul National University
Je-hyun Baek
Professor, Department of Mechanical Engineering, Pohang University of Science and Technology

A series of wind tunnel tests were conducted for Korean high-speed train model with various shape components to assess the contributions to aerodynamic drag. In order to elucidate the ground effects, two different wind tunnels, one with a moving ground system and the other with a fixed ground, were used for the same model and the results of both were compared and analyzed in detail. The results show that a suitable ground simulation is necessary for the test of a train model with many cars and detailed underbody. But the relative difference of the drag coefficients for the modifications of shape components can be measured by a fixed ground test with high accuracy and low cost. The effects of the nose shape, the inter-car gap and the bogie-fairing on total drag were discussed and some ideas were prosed to decrease the aerodynamic resistance of high speed train.

Key Words : High-speed Train, Aerodynamic Drag, Wind Tunnel Test

Nomenclature

C_D : Drag coefficient
$\overline{C}_D$: Mean drag coefficient
ΔC_D : Deviation of drag coefficient

1. Introduction

High-speed trains are running in Europe and Japan, and under construction in several countries including Korea as a new transportation system in the near future. Korean High-speed train is scheduled to run at the speed of 350km/h (about Mach number 0.27). At this high speed, aerodynamic drag is reported to amount 80% of the total drag. (Gawthorpe, 1975)

In the process of aerodynamic performance test of road vehicle including high-speed train, wind tunnel test can present the realistic data that are valid to real scale train. Furthermore, wind tunnel test enables to understand the flow mechanism of individual drag components, leading to aerodynamically advantageous shape.

Road vehicle has relative velocity to the ground that must be regarded in the wind tunnel test. To simulate this ground effect, various techniques including image method, ground plate, boundary layer suction, and tangential blowing (Wilemsen, 1997) have been developed, but a moving-belt ground plane (MBGP) (Peters, 1982, 1985) is highly recommended for some physical reason.

For zero yaw case a correct ground simulation can be obtained by moving the ground plane at the same velocity as the air flow relative to the train using a MBGP. In general, it is known that

* Corresponding Author,
E-mail : aerowolf@netian.com
TEL : +82-2-880-8051 ; **FAX** : +82-2-889-6205
Research Assistant, Department of Aerospace Engineering, Institute of Advanced Machinery Design, Seoul National University, Seoul 151-742, Korea.(Manuscript **Received** December 21, 1999 ; **Revised** August 18, 2000)

Table 1 *Specifications of subsonic wind tunnel of Flow Science*

Type	• closed return occupying 39 m×15 m floor space
Working Section	• 2.75 m×2.23 m octagonal cross section by 5.5 m long
Flow Details	• maximum test velocity 70 m/s • test section turbulence level<0.1%
Moving Ground	• maximum belt speed 60 m/s • platen dimensions 2. 67 m x 1.05 m(3.05 m between rollers) • capable of boundary layer removal. • separate suction control compartments

a MBGP is necessary for wind tunnel tests of relatively long body like the train with rough underbody.

This paper is on a series of the wind tunnel tests of Korean high-speed train. Tests were conducted in Flow Science subsonic wind tunnel (Manchester, U. K) with moving ground system and in POSTECH (Pohang University of Science and Technology) subsonic wind tunnel without moving ground system. We measured the drag of the train model to study the ground simulation technique. We also discussed the effects on total drag by the modification of train nose shape, inter-car shape and bogie fairing.

2. Wind Tunnel Test

2.1 Equipment

2.1.1 Subsonic wind tunnel of Flow Science (Manchester, U. K) : Moving belt ground plane

Subsonic wind tunnel of Flow Science is a closed loop type with 2.75m(W)×2.23m(H)×5.5m(L) test section and 2.67m long MBGP(Moving Belt Ground Plane). The maximum freestream velocity of the wind tunnel is 70m/s, but maximum test speed was restricted to the allowable belt speed, 60m/s. The details of the wind tunnel are described in Table 1 and the schematic of MBGP and the picture of the model installed in the test section is presented in Fig. 1 and 2 respectively.

In the moving ground wind tunnel, the model cannot be supported at the bottom, so 6-component internal balance was installed inside the model and connected to the strut which was fixed on the roof externally. As shown in Fig. 2, there is a suction slot in front of the MBGP which removes incoming upstream boundary layer to make uniform flow by adequate suction according to the freestream velocity and model size.

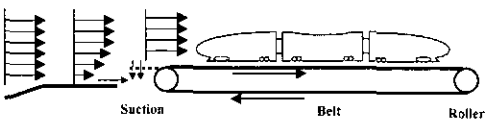

Fig. 1 Schematics of MBGP and suction system of *Flow Science subsonic wind tunnel*

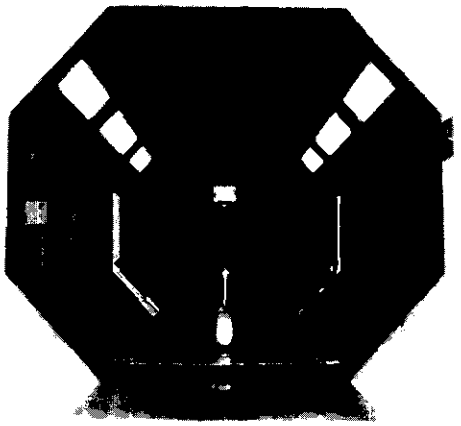

Fig. 2 Front view of the 1/20th scale model installed in the test section of Flow Science subsonic wind tunnel : 2.75 m(W)×2.23 m(H)×5.5 m(L)

2.1.2 POSTECH subsonic wind tunnel : Fixed ground

To compare the results of fixed ground measurement with those of moving ground measurement, and to investigate the drag of various shape

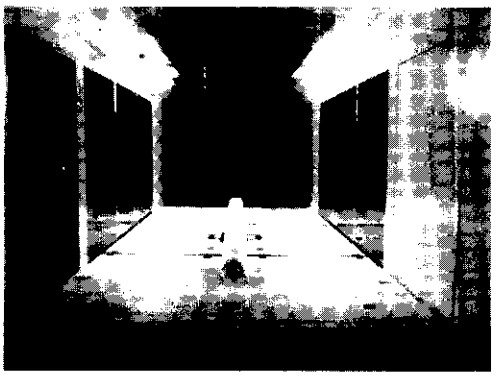

Fig. 3 Front view of the 1/20th scale model installed in the test section of POSTECH subsonic wind tunnel : 1.8m(W) × 1.5m(H) × 4.3m(L)

components, fixed ground test was conducted in subsonic wind tunnel of POSTECH. The dimension of the test section is 1.8m(W) × 1.5m(H) × 4.3m(L), and front view with installed model is shown in Fig. 3. To remove the incoming upstream boundary layer near the bottom of the test section, a ground plate was used on the height of 200mm from the bottom. By using the ground plate, the thickness of boundary layer at the nose of model reduced to 2mm. The model was installed on the external pyramidal balance at the bottom.

2.2 Test model

In general, the overall aerodynamic drag of train may be regarded as the sum of pressure drag and friction drag, where the skin friction drag is the sum of the longitudinal components of all the shear forces on the entire train surface and the pressure drag is the sum of the longitudinal components of all pressure forces on the entire train surface. Pressure drag is constant if the Reynolds number is larger than a critical Reynolds number which exist between 2×10^6 and 4×10^6(Peters, 1983), then measurements can be extrapolated to real train with high accuracy. Friction drag still depends on Reynolds number, but there are some compensations between surface roughness and Reynolds number effect. (Peters, 1985)

To get a supercritical Reynolds number, large scale model and high freestream velocity is needed. But, it is very hard because it needs a very costly compressed air, low temperature wind tunnel, or very large model that must e tested in a very large test section. In addition, a small model below the scale of 1/30 needs surface friction drag correction for the variation of the separation point. Considering these points, $1/30^{th}\sim1/10^{th}$ scale model is generally used in wind tunnel test of high-speed tunnel. (Peters, 1985)

Table 2 Specifications of the model

Scale	• 1/20
Cross Section	• 0.0224 m² (8.98 m² at real scale) • 139 mm(w) × 178 mm(h)
Total Length	• 2400 mm (48 m at real scale)
Ground Clearance	• 8.6 mm (172 mm at real scale)-European rail

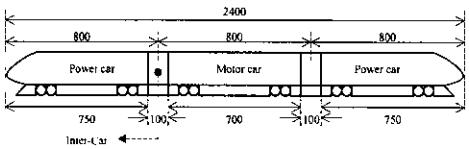

Fig. 4 Dimensions of the Model(mm)

Fig. 5 $1/20^{th}$ scale model installed in test section

2.2.1 Main features of the modular model

The length of the $1/20^{th}$ model is 2. 4m that corresponds to three-car train-set. The front car and rear car has identical nose shape at all configurations. The model is described in detail in Table 2 and Fig. 4. The picture of the model installed in test section is in Fig. 5. Figure 6 is the picture of the protrudent underbody of the model train with the bogie and wheels.

The modular model was partly exchangeable to compare the C_D deviation values by the modification of shape components. Two candidates of the nose shape proposed by SNU aerodynamic design team were used to survey the effect of the nose slenderness. For inter-car shape, two models with conventional gap (500mm at real scale) as well as

without gap were tested in order to assess the effect of the gap. The model has six bogies and bogie fairing can be attached to each bogie at ease. Table 3 and Fig. 7 show detailed description and schematics of the variations of the test model

Table 3 Modifications of the shape components

Module	Modification
Nose(Power car)	• Nose1 : long nose (nose slenderness : 2.0) • Nose2 : shor nose (nose slenderness: 1.6)
Inter-car	• Inter1 : 25mm gap • Inter2 : no gap
Bogie fairing	• Fairing1 : fairing on first bogie on both of the end (OXXXXO) • Fairing2 : no fairing (XXXXXX) • Fairing3 : fairing on first and second bogie (OOXXOO) • Fairing4 : fairing on all bogie (OOOOOO)

Fig. 6 Under body of the test model (bogie, wheel, and bogie fairing)

2.2.2 The configuration of the test model

Basic configuration was composed of Nose 1, Inter 1, Fairing 1 which were most probable candidates for the future Korean high-speed train. Then the combination with the Nose 2, Inter 2 and Fairing 2 led to a lot of variations, and each variation was named as Nvari, Ivari, Fvari and NIvari, NFvari, etc. The combination of each shape component in Table 3 resulted in sixteen train configurations. But fairing 3 and fairing 4 were combined with only Nose 1 and Inter 1. So total number of test configurations reduced to ten as shown in Table 4 for the test without moving belt.

Test on moving belt costs much more than fixed ground, so moving ground tests were restricted to

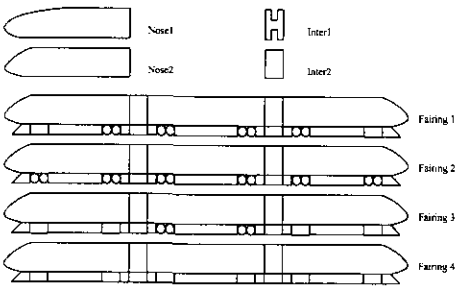

Fig. 7 Modifications of the shape components

Table 4 Configurations of the model

Configuration name	Nose type	Inter-car type	Bogie Fairing type
Basic	Nose1	Inter1	Fairing1
Nvari	Nose2	Inter1	Fairing1
Ivari	Nose1	Inter2	Fairing1
Fvari	Nose1	Inter1	Fairing2
NIvari	Nose2	Inter2	Fairing1
IFvari	Nose1	Inter2	Fairing2
NFvari	Nose2	Inter1	Fairing2
NIFvari	Nose2	Inter2	Fairing2
FFvari	Nose1	Inter1	Fairing3
FFFvari	Nose1	Inter1	Fairing4

Table 5 Experimental condition of Flow Science wind-tunnel.

Test name	Model Name	Velocity(m/s)	Moving Belt
Basic test	Basic	40/60	On
Nose type test	Nvari	40/60	On
Bogie fairing test	Fvari	40/60	On

Table 6 Total CD and deviation relative to the CD of Basic configuration(moving ground)

Model name	C_D	$\Delta C_D/_{,basic}$(%)
Basic	0.421591	0.0
Nvari	0.456249	8.2
Fvari	0.449374	6.6

only three configurations Basic, Nvari, Fvari. (shaded at Table 4). But on fixed ground condition, all of the ten configurations were tested and analyzed.

2.2.3 Test condition

To acquire resonable Reynolds number, the freestream velocity was set up at 60m/s that was the maximum speed of moving belt. In this condition, the effective Reynolds number is supercritical region, that the measurement can be extrapolated to real train with high accuracy. (Peters, 1985)

As shown in Table 5, tests in moving-belt wind tunnel were carried out for three configurations (basic, Nvari, and Fvari) under the condition of freestream velocity 40m/s and 60m/s. But on the fixed-ground wind tunnel, all of the ten configurations were tested with freestream speed varying from 30m/s to 60m/s with 10m/s interval.

2.2.4 Measurements system and data reduction

In Flow Science windtunnel test, drag force was measured by 6-component internal balance installed inside the model. The internal balance was connected to the strut which was supported to the frame outside of the ceiling of the test section. Separately measured three drag force of each car was added to attain total drag coefficient. (Gaylard, 1995) In POSTECH windtunnel test,

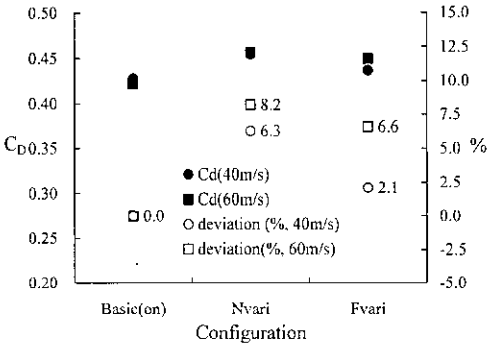

Fig. 8 Total C_D and deviation by the combination of shape component(moving ground)

6-component external balance was used to measure total drag at one time. Unlike the moving ground test, balance was under the test section that is a general setup of conventional wind tunnel.

The measured drag force, D was reduced to the drag coefficients C_D, as follows,

$$C_D=\frac{D}{qS}$$

where q represents the dynamic pressure of the relative wind($q=\frac{1}{2}\rho v^2$, with ρ being the flow density and v the relative wind speed) and S is the reference area(projected frontal area).

3. Experimental Results

3.1 Results in moving-ground wind tunnel

Table 6 and Fig. 8 show the drag coefficient, C_D, and the C_D deviation, ΔC_D, relative to that of Basic configuration on the moving ground test. The drag coefficient of short nose(Nvari configuration) was 8.2% larger than long nose(Basic configuration) and the removal of the bogie fairing(Fvari configuration) increases the drag by 6.6% compared with the basic configuration at

Table 7 Measured total C_D(fixed ground)

Model name / V(m/s)	Basic	Nvari	Ivari	Fvari	NIvari	IFvari	NFvari	NIFvari
30	0.372	0.403	0.357	0.399	0.392	0.385	0.430	0.420
40	0.368	0.397	0.352	0.388	0.386	0.379	0.424	0.416
50	0.360	0.393	0.346	0.381	0.380	0.371	0.419	0.412
60	0.359	0.389	0.342	0.380	0.377	0.364	0.416	0.406
$\Delta C_D/C_{D,basic}$ (%)	0.00	8.49	-4.29	6.11	5.26	2.82	15.74	13.41

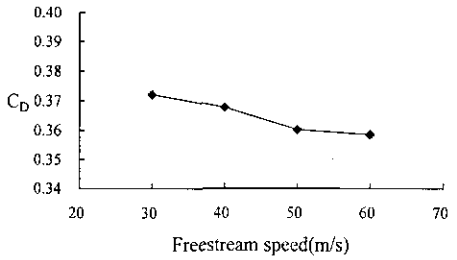

Fig. 9 Drag coefficient variation with freestream velocity(Basic model)

freestream speed 60m/s. When the freestream speed was reduced to 40m/s, drag coefficients coincided very well with results at 60m/s except Fvari(2.1%, 40m/s). As will be shown next, Fvari configuration reduced drag coefficient by 6.11% on the fixed ground test and this was very close to the result of moving-ground test at 60m/s.

3.2 Results in fixed-ground wind tunnel

The test results on fixed ground are shown at Table 7. To investigate the effect of Reynolds number on the drag coefficient, drag coefficients relative to the freestream velocity are plotted in Fig. 9. As shown in the figure, drag coefficients were found to converge to a constant value as freestream velocity gets larger than 50m/s. This results confirms that when the freestream velocity was over 50m/s, the Reynolds number was above the critical Reynolds number and therefore the test results were meaningful to be adapted to real-scale train.

The drag coefficient, 0.359 of the Basic model on fixed ground(Table 7) showed a good comparison with the moving-ground test result, 0.410 (Table 6). The difference of drag by 12.4% resulted from the ground condition.

Table 8 C_D deviation by shape modification(moving ground)

Modified Shape component	ΔC_D	$\Delta C_D/C_D$ (%)
Nose	0.035	8.2
Bogie fairing	0.028	6.6

This is mainly due to the dramatic alteration of the flow under the model by the presence of the moving ground. When a train runs on the ground, there are relative velocity between a train and the ground so that the vehicle undergoes large aerodynamic drag due to the complex shape of underbody(Fig. 6). With a conventional fixed ground condition, air, passing under the vehicle model, reduces in its velocity due to both frictional effects and the blockage effect by the stationary ground, leading to a small aerodynamic drag.

Peters(1986) found that using a MBGP increased C_D values by 30% for a $1/5^{th}$ scale short maglev vehicle with a smooth underbelly and only 20mm (full scale) ground clearance. It is expected that the errors in C_D involved in the test using a fixed ground will be greater for longer models, so MBGP is necessary for the test of the train model with many cars and detailed underbody.

3.3 The effect of the shape components on

C_D values of the each configuration and their deviations by the modification of the shape component are shown at the Table 8 and Table 9. The interaction between the shape components on C_D was not considered because only three configurations were tested on moving ground, while all available configurations were tested to investigate

Table 9 C_D deviation by shape modification (fixed ground)

(a) C_D diviation by the modification of mose shape

Inter-car	Fairing	ΔC_D	$\Delta C_D/\overline{C_D}$ (%)
Inter1	Fairing1	0.031	8.58
Inter2	Fairing1	0.035	10.29
Inter1	Fairing2	0.036	9.44
Inter2	Fairing2	0.042	11.53
Average		0.036	9.96

(b) C_D deviation by the modificatioin of inter-car

Nose	Fairing	ΔC_D	$\Delta C_D/\overline{C_D}$ (%)
Nose1	Fairing1	-0.016	-4.56
Nose2	Fairing1	-0.012	-3.05
Nose1	Fairing2	-0.015	-4.08
Nose2	Fairing2	-0.009	-2.25
Average		-0.013	-3.48

(c) C_D deviation by the modificatioin of bogie fairing

Nose	Inter-car	ΔC_D	$\Delta C_D/\overline{C_D}$ (%)
Nose1	Inter1	0.021	5.92
Nose2	Inter1	0.026	6.76
Nose1	Inter2	0.022	6.45
Nose2	Inter2	0.029	7.64
Average		0.025	6.69

the interaction in the fixed-ground test.

As shown in Table 8, C_D increased 0.035 that corresponded 8.22% of the total C_D by changing the nose shape. C_D of no-bogie-fairing configuration (Fvari) also increased by 0.028 which was 6.59% of the basic configuration's C_D value.

The C_D deviation by the modification of one shape component can be affected by the combination of other shape components. In the fixed-ground wind tunnel test, full matrix of the shape components were tested, so it was possible to examine the aerodynamic interaction between the shape components. As shown in Table 9, the C_D deviation value can be calculated from four data sets. For example, the effect of the modification of nose on C_D value may be measured at four cases

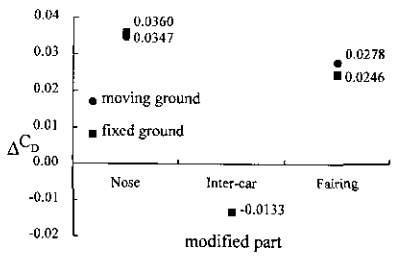

Fig. 10 ΔC_D by the modification of shape component

by the combination of Inter-car and bogie fairing. In Table 9, the four deviation values in reference to the modification of each shape component approach to their average value with maximum error of about 2% of the total C_D. From the results above, we assume that the interaction between shape components was almost negligible in this test, because the quantity of the error was almost the same as the balance resolution. This means that each average value of four C_D deviation values can be used to assess the contributions of the shape components to total aerodynamic drag.

Beside the aerodynamic independency between the shape components, another feature can be found by comparing two results in Fig. 10 that illustrates the C_D deviation relative to the modification with and without MBGP. By the modification of nose shape each deviation value approached to 0.035 with MBGP and 0.036 without MBGP. When bogie fairing is concerned, the C_D deviation between Basic and Fvari configuration was 0.028 with MBGP and 0.025 without MBGP, in which the deviation was slightly larger because bogie and bogie fairing was near the ground and the measurement was more affected by ground condition.

From the results above, we can conclud that fixed-ground wind tunnel can be used to estimate the relative deviations of drag by the modifications of shape component with good accuracy with less effort, even if it fails to catch the total drag of train model.

Table 8 and Table 9 also show the contributions by the modification of each shape component to total aerodynamic drag. The long nose type of slenderness 2 (Nose 1) marked less C_D by

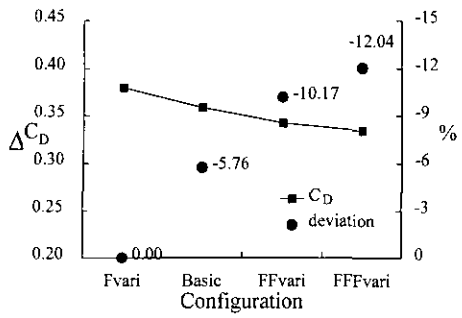

Fig. 11 C_D variation by the bogie fairing configuration

0.036(9.96% of total C_D) than the short nose type of slenderness 1.6(Nose 2). The smaller aerodynamic drag seems to originate not only from the low pressure drag of the front nose but also from the good pressure-recovery around the rear nose.

It is well known that the minimization of pressure wave generated when a train is entering into a tunnel is more important than minimization of aerodynamic drag. (Peters, 1985) Generally longer nose is advantageous for the minimization of compression wave and in addition, the results of the wind tunnel test show that longer nose shape also decreases aerodynamic drag. So, we conclude that the larger slenderness of the train nose is recommendable not only for the reduction of compression wave but also for the countermeasure of the aerodynamics drag of high-speed train.

Conventional inter-car shape(500mm gap at real scale) marked C_D about 0.013(3.48% of total C_D) which was less than half of the contribution of nose component. But, in real train the portion of inter-car will be far larger ; i. g. for a twenty-car train-set, the number of inter-car gap is 19 and the C_D portion of the gap is 0.1235 which is about three times of the contribution from the modification of nose shape. This means that covering the inter-car gap can reduce aerodynamic drag more efficiently.

Figure 11 shows the total C_D value for different configurations of bogie fairing. Total C_D decreases as the number of bogie fairing increases and then all of the bogies were covered(Faring4), the total C_D decreases by 12% relative to no-bogie fairing configuration(Fairing2) in present three-car train model. First and second bogie fairing at both end leaded to reduction of total C_D by 5.76% and 4.93% respectively, but third bogie reduced C_D only by 1.87%. From the result above, we can confirm that the first and second bogie fairings play siginificant roles to diminishing the underbody flow, as well as to reduce the drag induced by the protrudent bogie system.

4. Conclusions

A series of wind tunnel test were conducted with $1/20^{th}$ scale three-car model of Korean high-speed train in two different wind tunnel with and without moving ground system. The effects of the wind tunnel ground condition were carefully observed. Changing the model shape components such as nose shape, inter-car, and bogie fairing, their effects on drag were also surveyed. From the results we can conclude that :

(1) Moving ground is necessary for wind tunnel test of long road vehicle like train to measure the aerodynamic drag accurately. In this experiments, about 12% less C_D was measured on fixed ground relative to moving ground for three-car model.

(2) Fixed-ground test can measure the relative deviations by the modifications of shape components fairly good with less effort.

(3) Little interaction between shape components was found in the fixed-ground test.

(4) Slender nose(Nose1) reduced C_D by about 10% relative to blunt nose(Nose2) in the present study, because of not only low surface pressure on front nose but also good recovery of wake pressure on rear nose.

(5) Each inter-car gap contributed 3.5% of the total C_D . Covering the inter-car gap can reduce aerodynamic drag and the effect gets higher as the number of car gets larger.

(6) The fairing on protrudent bogie can reduce C_D by up to 12%. The first and second bogie fairings for both ends had dominant effect on drag reduction.

(7) Aerodynamic design optimization leads to the reduction of aerodynamic drag, which is very

worthwhile from an economic point of view.

Acknowledgements

This study is a result of 'R&D Project for High speed Railway system' by the financial supports from the government of Republic of Korea. And, IAMD in S. N. U. contributed to this study with administrative aid and facilities.

References

Gawthorpe, R. G., 1975, "Energy Consumption at High Speed", Railway Gazette International

Wilemsen, E., 1997, "High Reynolds Number Wind Tunnel Experiments on Trains", *Journal of Wind Eng. and Ind. Aerodynamics*, 69-71 pp. 437~447.

Peters, J-L, 1982, "Optimising Aerodynamics to Raise IC Perfomance", Railway Gazette International, 1982, 10, pp. 817~819.

Jean-Luc Peters, 1983, "Aerodynamics of Very High Speed Trains and Maglev Vehicles : State of the Art and Future Potential", *Int. J. of Vehicle Design*, Special Publication Sp3.

Jean-Luc Peters, 1985, "Aerodynamische Gestaltung von Schienenfahrzeugen fur den schnellverkerhr", AET(40)

Jean-Luc Peters, 1986, "Influence of Moving Ground Belt on the Aerodynamic Drag of Wind Tunnel Models", *Presentation 3D workshop on the aerodynamic drag of trains*, Derby, UK, 8-9 April 1986.

Lee, D. H., et al., 1998, "Second year Report of Aerodynamic Design and analysis of Korean HST project".

Kim, I. S. Chung, J. D. Choi, S. W., 1997, " Computational and Experimental Investigation of the Flowfields About High Speed Train Configurations", *KSAS Journal*, Vol. 25 No. 6 pp. 56~65.

Tyll, J. S., et al., 1996, "Experimental Studies of Magnetic Levitation Train Aerodynamics", *AIAA Journal* Vol. 34 No. 12.

Mercker, E., Knape, H. W., 1989, "Ground Simulation with Moving Belt and Tangential Blowing for Full-Scale Automotive Testing in an Wind Tunnel", SAE Paper 890367

Mercker, E., Wiedemann, J., 1990, "Comparison of Different Ground Simulation Techniques for Use in Automotive Wind Tunnels", SAE Paper 900321.

Kang, S. H., Lee, D. H., et al., 1988, "Experimental Studies on the Estimation of Wind-Load of a Container Crane and Its Development", *KSME Interational Journal*, vol. 12, No. 4, pp. 892~899.

Gaylard, A. P., Howlett, A. B., Harrison, D. J., 1995, "Assessing Drag Reduction Measures for High-Speed Train", BRR Report.